Extending matchgates to universal quantum computation via the Hubbard model

Jia-Wei Ji[*] and David L. Feder [†]

Institute for Quantum Science and Technology, University of Calgary, Alberta T2N 1N4, Canada

Quantum circuits solely comprising matchgates can perform nontrivial (but nonuniversal) quantum algorithms. Because matchgates can be mapped to noninteracting fermions, these circuits can be efficiently simulated on a classical computer. Universal quantum computation is attainable by adding any nonmatchgate parity-preserving gate, from which one may infer that interacting fermions are natural candidates for universal quantum computation. We consider the quantum computational power of fermions hopping on a one-dimensional double-well lattice within the context of matchgates. In particular, we show that universal quantum computation can be implemented using spinless (spin-polarized) fermions and nearest-neighbor interactions, as well as with spin-half fermions with on-site interactions (i.e., the Hubbard model). We suggest that these schemes are currently within reach in the context of ultracold atomic gases.

I. INTRODUCTION

Matchgates, first proposed by Valiant, are a special class of two-qubit quantum gates that can perform nontrivial quantum algorithms but are not universal [1]. Quantum circuits composed of these quantum gates defined in the context of graph theory can be efficiently simulated on a classical computer if they just act on nearest-neighbor qubits. Matchgates can be extended to universal quantum computation (UQC) by adding the SWAP operation [2] or any parity-preserving nonmatchgate unitary [3].

Matchgates physically correspond to noninteracting fermions in one dimension [4–6], implying that simulating noninteracting fermions is also classically efficient. Indeed, the state of noninteracting fermions is described by a determinant which can be evaluated in polynomial time. The efficient classical simulatability of noninteracting fermions remains even with adaptive measurements of fermion occupation [4]. Fascinatingly, encoding the quantum information in the fermion spin while performing measurements on the spatial locations allows for universal quantum computation [7].

These results suggest that interacting fermions could be natural candidates for universal quantum computation. In fact, UQC is achievable in principle with interacting Majorana fermions [8,9]. While Majorana fermions have the advantage of topologically protecting the quantum information from errors, they are difficult to realize in the laboratory. So far, few experiments have unequivocally observed Majorana fermions, let alone control and manipulate them [10,11]. Nevertheless, these systems hold such promise that currently there is a large push toward their experimental realization [12].

In this work, we study the possibility of realizing UQC with conventional interacting fermions, within the matchgate formalism. Conventional fermions are not topologically protected, but are much easier to confine and manipulate in the laboratory. Due to the Pauli principle, spinless fermions would require at least nearest-neighbor interactions; however, controlling Coulomb or dipole-dipole interactions in the laboratory is not necessarily straightforward. We therefore consider the Hubbard model [13], which describes spin-1/2 fermions hopping between neighboring sites of a lattice and repulsive on-site interactions between particles with opposite spin projection. The Hubbard model has been used to describe a wide variety of condensed matter systems [14], with particular success in high-temperature superconductivity [15,16], and has been recently realized experimentally by confining ultracold fermionic atoms in optical lattices [17].

We consider a variant of the Hubbard model in a one-dimensional double-well lattice, where qubit registers correspond to the fermionic occupation of sites within a given double well. The time evolution under local potentials and intersite hopping effects single-qubit gates, and maps the system to matchgate circuits. Two-qubit gates that extend the model beyond matchgate circuits result from interactions between fermions. We first consider spinless (or spin-polarized, single-component) fermions for simplicity. Inducing nearest-neighbor interactions can yield two-qubit (controlled-PHASE) gates, which elevates the matchgates to universal quantum circuits. We discuss the feasibility of implementing this strategy with ultracold atoms in optical lattices; while most aspects are well within reach of current experimental capability, the requirement of inducing time-dependent nearest-neighbor interactions is expected to be a challenge. We therefore consider the Hubbard model, which features spin-half fermions and therefore allows on-site interactions. Surprisingly, we find that entangling gates are never possible in this model if the hopping amplitudes are assumed to be spin independent. Allowing spin-dependent hopping enables two-qubit gates for a wide range of parameters. Given that spin-dependent optical lattices have been realized experimentally in the context of ultracold atomic gases, we expect that this approach could be a

————————
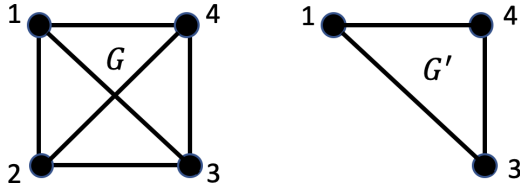[*]jiawei.ji@ucalgary.ca
[†]dfeder@ucalgary.ca

FIG. 1. The complete graph G and the graph G' resulting from deleting the omittable node $T = \{2\}$. The input and output nodes are $X = \{1\}$ and $Y = \{4\}$, respectively.

promising avenue for the realistic implementation of universal (small-scale) quantum algorithms.

Section II reviews the definitions of matchgates and their relationship with noninteracting fermions. Section III then considers the power of spinless (or spin-polarized) fermions on a double-well lattice to perform universal quantum computation with the addition of nearest-neighbor interactions, and discusses the feasibility of implementing the procedure using ultracold atoms in optical lattices. Given possible experimental challenges, the Hubbard model for spin-half fermions is explored in Sec. IV, where we show that universal quantum computation is only possible with one-dimensional lattices if the hopping amplitudes are spin dependent.

II. REVIEW

A. Perfect matchings and matchgates

Matchgates are defined in the context of the perfect matchings in graph theory [1]. In a connected graph G, with an even number $2k$ of vertices, a matching is perfect if it contains k edges and these k edges share no vertices. The Pfaffian can be defined as a sum of all the possible perfect matchings, with each perfect matching modified by the parity of the number of overlapping pairs.

In Fig. 1, the Pfaffian of the graph G is

$$\mathrm{Pf}(G) = w_{14}w_{23} + w_{12}w_{34} - w_{13}w_{24}, \qquad (1)$$

where w_{ij} is the weight assigned to the edge connecting the nodes i and j. The negative sign in the last term of the Pfaffian arises from the overlap of the two edges (1,3) and (2,4). The skew-symmetric matrix B associated with A is

$$B = \begin{pmatrix} 0 & w_{12} & w_{13} & w_{14} \\ -w_{12} & 0 & w_{23} & w_{24} \\ -w_{13} & -w_{23} & 0 & w_{34} \\ -w_{14} & -w_{24} & -w_{34} & 0 \end{pmatrix}. \qquad (2)$$

The determinant of this matrix is

$$\det(B) = (w_{14}w_{23} + w_{12}w_{34} - w_{13}w_{24})^2, \qquad (3)$$

which is the square of the Pfaffian.

Since the determinant can be computed on a classical computer in time $O(n^{2.373})$, where n is the dimension of the matrix, the Pfaffian is also efficiently computable. If n is odd, the corresponding Pfaffian is simply zero which could be understood in the light of the perfect matchings: If there are an odd number of nodes in graph then it is impossible to pair them all.

The Pfaffian sum is defined as the sum of Pfaffians of all possible sizes,

$$\mathrm{PfS}(G) = \sum_{S} \mathrm{Pf}(G - S), \qquad (4)$$

where $S \subseteq T$, and T is a set of omittable nodes in the graph G (the choice of T is arbitrary). In Fig. 1, choosing node 2 of G as omittable yields graph G' (with node 2 removed). The Pfaffian sum of the graph G is, then,

$$\mathrm{PfS}(G) = \mathrm{Pf}(G) + \mathrm{Pf}(G'). \qquad (5)$$

Evidently, $\mathrm{Pf}(G') = 0$ because it has an odd number of nodes.

The character matrix of a matchgate Γ is defined as

$$\chi(\Gamma, Z) = \mu(\Gamma, Z)\mathrm{PfS}(G'), \qquad (6)$$

where $Z \subseteq X \cup Y$ are external nodes. The input and output nodes of the graph G are $X \subseteq V, Y \subseteq V$, and $G' = (V - Z, E', W')$ is the graph with external nodes Z and corresponding edges deleted from the graph G. The modifier $\mu(\Gamma, Z) = \pm 1$, depending on the number of overlaps between E' and the external edges. In the literature, the matchgate corresponds to the character matrix χ.

Consider again the graph G in Fig. 1. Suppose that one chooses two external nodes, $Z = \{1, 4\}$. This might correspond to a single-qubit gate, for example. Following the previous steps, one obtains

$$\begin{aligned} a &= \chi(\Gamma, \emptyset) \\ &= w_{23}w_{14} - w_{13}w_{24} + w_{12}w_{34}; \\ b &= \chi(\Gamma, \{1\}) = w_{34}; \\ c &= \chi(\Gamma, \{4\}) = w_{13}; \\ d &= \chi(\Gamma, \{1, 4\}) = w_{23}. \end{aligned} \qquad (7)$$

This yields the character matrix,

$$\chi(\Gamma, Z) = \begin{array}{c} \\ \emptyset \\ 1 \end{array} \begin{pmatrix} \emptyset & 4 \\ a & b \\ c & d \end{pmatrix}. \qquad (8)$$

For a (larger) graph with four external nodes, a 4 by 4 character matrix or matchgate can be obtained. Satisfying Valiant's five identities [1], the matchgate is generally expressed as [2,4]

$$G(A, B) = \begin{pmatrix} A_{11} & 0 & 0 & A_{12} \\ 0 & B_{11} & B_{12} & 0 \\ 0 & B_{21} & B_{22} & 0 \\ A_{21} & 0 & 0 & A_{22} \end{pmatrix}, \qquad (9)$$

where $\det(A) = \det(B)$ and $A, B \in U(2)$. Designating the four possible inputs as $\{|00\rangle, |01\rangle, |10\rangle, |11\rangle\}$, matchgates are a special class of two-qubit quantum gates, in which the even-parity subspace $\{|00\rangle, |11\rangle\}$ and odd-parity subspace $\{|01\rangle, |10\rangle\}$ are completely decoupled. If these two-qubit matchgates act only on nearest-neighbor qubits, then any quantum circuit composed of them can be efficiently simulated classically [1].

Matchgates can generate entanglement, which implies that quantum circuits comprising them yield classically nontrivial states in spite of their being efficiently simulatable classically. These quantum circuits can be elevated to UQC if any

nonmatchgate parity-preserving gate is added [2], such as SWAP [3]. The SWAP gate $G(I, X)$ is not a matchgate because $\det(I) = -\det(X)$; it is matchgate equivalent to the maximally entangling controlled-PHASE (CZ) gate via the transformation $CZ = G(Z, I) = G(H, H)G(X, X)G(I, X)G(H, H)$. The power of the SWAP gate in this context can be readily understood by considering the fermionic representation of matchgates, discussed in the next section.

B. Matchgates and noninteracting fermions

In quantum field theory, Wick's theorem is frequently used to approximate the expectation value of a string of fermionic field operators, by reducing it to products of operator pairs:

$$\langle 0|A_1...A_{2n}|0\rangle = \sum (\pm 1)^{\mathrm{p}}\langle A_{i_1}A_{j_1}\rangle...\langle A_{i_n}A_{j_n}\rangle, \quad (10)$$

where the sum runs over all possible permutations of indices $1...2n$ and p is the number of permutations that take $1...2n$ to $i_1, j_1...i_n, j_n$. The phase accounts for fermionic statistics. Evidently, this expectation value is zero unless there is an even number of operators, implying that all operators must be perfectly matched (paired). Consider the case with four operators:

$$\langle A_1 A_2 A_3 A_4 \rangle = \langle A_1 A_2 \rangle\langle A_3 A_4 \rangle - \langle A_1 A_3 \rangle\langle A_2 A_4 \rangle$$
$$+ \langle A_1 A_4 \rangle\langle A_2 A_3 \rangle, \quad (11)$$

which has the same form as the Pfaffian of the graph G [Eq. (1)]. A similar approach was used to evaluate the output probabilities for a fermionic quantum circuit [4].

The close relationship between fermions and Pfaffians reflects the fact that in first quantization fermionic wave functions are described by Slater determinants. Indeed, it is well understood that the classical simulation of fermionic linear optics is efficient [4–6], in marked contrast to the bosonic case [18].

More important for the present work, matchgates can be directly constructed directly via noninteracting fermions. The general number-conserving Hamiltonian for two fermionic modes or sites is

$$H = -t f_i^\dagger f_j - t f_j^\dagger f_i - \mu_i f_i^\dagger f_i - \mu_j f_j^\dagger f_j, \quad (12)$$

where f_i ($f_i^\dagger$) annihilates (creates) a fermion at site i, $-t$ is the amplitude to hop between the ith and jth sites ($t > 0$), and μ_i and μ_j are local chemical potentials on sites i and j. The number conservation follows from the vanishing of the commutator $[H, n] = 0$, where the total number operator is $n = f_i^\dagger f_i + f_j^\dagger f_j$. This can be easily verified using the fermionic algebra,

$$\{f_i, f_j^\dagger\} = \delta_{ij}; \quad \{f_i, f_j\} = \{f_i^\dagger, f_j^\dagger\} = 0, \quad (13)$$

where $\{\ldots, \ldots\}$ represents an anticommutator. The complete fermionic Fock or occupation basis for two sites corresponds to $|x_1\rangle = |\emptyset\rangle$, $|x_2\rangle = f_i^\dagger|\emptyset\rangle$, $|x_3\rangle = f_j^\dagger|\emptyset\rangle$, and $|x_4\rangle = f_i^\dagger f_j^\dagger|\emptyset\rangle$. The Hamiltonian is then expressed as

$$H = \begin{pmatrix} 0 & 0 & 0 & 0 \\ 0 & -\mu_i & -t & 0 \\ 0 & -t & -\mu_j & 0 \\ 0 & 0 & 0 & -\mu_i - \mu_j \end{pmatrix}, \quad (14)$$

where each block corresponds to a fixed particle number. The time evolution of the system under this Hamiltonian is given by the unitary matrix,

$$e^{-iH\tau} = \begin{pmatrix} 1 & 0 & 0 & 0 \\ 0 & b_{22} & b_{23} & 0 \\ 0 & b_{32} & b_{33} & 0 \\ 0 & 0 & 0 & e^{it(\mu_i+\mu_j)} \end{pmatrix}, \quad (15)$$

where τ is the time variable, and the middle block is the exponential of the corresponding block in the Hamiltonian. For this to be a matchgate, one requires

$$\det\begin{vmatrix} b_{22} & b_{23} \\ b_{32} & b_{33} \end{vmatrix} = e^{i(\mu_i+\mu_j)\tau}. \quad (16)$$

Using Jacobi's identity $\det(e^{sB}) = e^{\mathrm{tr}(sB)}$, where s is a scalar and B is a matrix, one immediately obtains

$$\det\begin{vmatrix} b_{22} & b_{23} \\ b_{32} & b_{33} \end{vmatrix} = \exp\left[-i\tau\,\mathrm{tr}\begin{pmatrix} -\mu_i & -t \\ -t & -\mu_j \end{pmatrix}\right] = e^{i(\mu_i+\mu_j)\tau}. \quad (17)$$

Therefore, this Hamiltonian yields a matchgate.

Consider a more general number nonpreserving Hamiltonian:

$$H' = H + \tilde{t} f_i f_j + \tilde{t}^* f_j^\dagger f_i^\dagger, \quad (18)$$

where evidently now $[H', n] \neq 0$. In the Fock basis one obtains

$$H' = \begin{pmatrix} 0 & 0 & 0 & \tilde{t} \\ 0 & -\mu_i & -t & 0 \\ 0 & -t & -\mu_j & 0 \\ \tilde{t}^* & 0 & 0 & -\mu_i - \mu_j \end{pmatrix}, \quad (19)$$

which is block diagonal with row and column permutations. The evolution operator can then be written,

$$e^{-iH'\tau} = \begin{pmatrix} a_{11} & 0 & 0 & a_{14} \\ 0 & b_{22} & b_{23} & 0 \\ 0 & b_{32} & b_{33} & 0 \\ a_{41} & 0 & 0 & a_{44} \end{pmatrix}. \quad (20)$$

Applying Jacobi's identity twice, one obtains

$$\det(\mathbf{a}) = \det(\mathbf{b}) = e^{i(\mu_i+\mu_j)\tau}, \quad (21)$$

which demonstrates that this gate is also a matchgate.

Quadratic Hamiltonians like Eq. (18) can always be diagonalized into the form,

$$H' = \lambda_i c_i^\dagger c_i + \lambda_j c_j^\dagger c_j, \quad (22)$$

using a local Bogoliubov transformation of the form,

$$c_k = \alpha_k f_k + \beta_k^* f_k^\dagger, \quad (23)$$

with λ, α, and β complex coefficients. A special choice of these parameters corresponds to Majorana fermions, defined by

$$c_{2i} = f_i + f_i^\dagger; \quad c_{2i+1} = -i(f_i - f_i^\dagger); \quad \{c_k, c_l\} = 2\delta_{kl}. \quad (24)$$

These operators are Hermitian, i.e., $c_{2i} = c_{2i}^\dagger$ and $c_{2i+1} = c_{2i+1}^\dagger$, so that Majorana fermions are their own antiparticles. Noninteracting Majorana fermions are efficiently simulatable
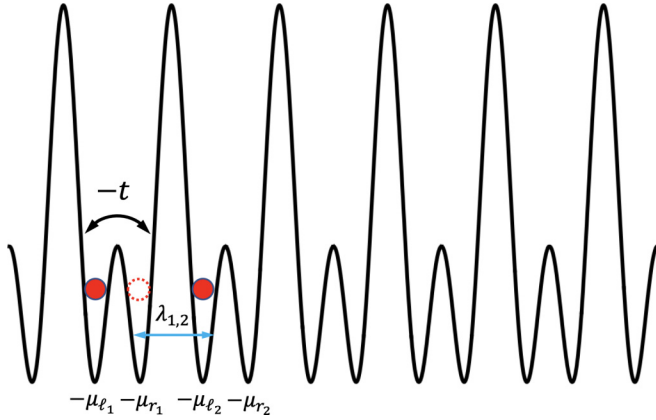
FIG. 2. The double-well lattice potential for spinless fermions. Each successive double well contains at most one fermion. Hopping with amplitude t is only permitted between sites of a given double well j. Local potentials in the left (ℓ) and right (r) sites are denoted by μ_{ℓ_j} and μ_{r_j}, respectively. The nearest-neighbor interaction strength between sites i and j is $\lambda_{i,j}$.

classically [4], a result that follows directly from the underlying quadratic Hamiltonian, but the addition of quartic interactions allow for UQC [8].

III. SPINLESS FERMIONS

A. Single-qubit operations

Given the Hamiltonian for fermions in two modes or sites, Eq. (12), it is convenient to encode quantum information in the odd-parity subspace of the matchgate,

$$|0\rangle_L = |10\rangle = f_\ell^\dagger |\emptyset\rangle, \quad |1\rangle_L = |01\rangle = f_r^\dagger |\emptyset\rangle, \qquad (25)$$

where a fermion on the left (ℓ) and right (r) sites are encoded as logical states $|0\rangle_L$ and $|1\rangle_L$, respectively. This is in contrast with previous (Majorana fermion) schemes in which the encoding is in the even-parity subspace [2,3]. Figure 2 depicts a possible arrangement of qubits in a one-dimensional double-well lattice. Each successive double-well potential contains a single fermion and thereby encodes a qubit. The potential barrier between double wells is assumed to be so large that no fermionic tunneling is possible between different double-well potentials.

Within a given double-well potential, the Hamiltonian is

$$H = \begin{pmatrix} -\mu_\ell & -t \\ -t & -\mu_r \end{pmatrix}, \qquad (26)$$

where $t \in \mathbb{R}$ stands for the hopping strength between left and right sites, and μ_ℓ and μ_r are possible local potentials. This can be rewritten as

$$H = -tX + \frac{-\mu_\ell + \mu_r}{2}Z - \frac{\mu_\ell + \mu_r}{2}I, \qquad (27)$$

where X, Z, and I are Pauli matrices. Time evolution under this Hamiltonian yields

$$U = \exp\left\{ i\left[tX + \frac{\mu_\ell - \mu_r}{2}Z + \frac{\mu_\ell + \mu_r}{2}I \right]\tau \right\}. \qquad (28)$$

A straightforward calculation yields the explicit expression,

$$U = e^{i(\mu_\ell + \mu_r)\tau/2}\left\{ \cos(\omega\tau)I + \frac{i}{\omega}\sin(\omega\tau)\left[tX + \frac{\mu_\ell - \mu_r}{2}Z \right] \right\}, \qquad (29)$$

where

$$\omega = \sqrt{t^2 + \left(\frac{\mu_\ell - \mu_r}{2} \right)^2}.$$

Combinations of these, with different choices of local potentials and evolution time (fixing the intersite tunneling amplitude t) can yield any desired single-qubit unitary gate. Particularly useful cases correspond to $t = 0$,

$$U(t = 0) = \text{diag}(e^{i\mu_\ell \tau}, e^{i\mu_r \tau}), \qquad (30)$$

which gives a rotation around the Z axis by an angle $\omega = (\mu_r - \mu_\ell)\tau/2$ up to an unimportant overall phase; and to $\mu_\ell = \mu_r$,

$$U(\mu_\ell = \mu_r) = e^{i\mu_r \tau}[\cos(t\tau)I + i\sin(t\tau)X], \qquad (31)$$

corresponding to a rotation around the X axis by an angle $-t\tau$ again up to an unimportant phase.

Successive rotations around these orthogonal axes are sufficient to yield any single-qubit gate. Once the desired gate is implemented, intersite hopping is quickly quenched by adding a strongly repulsive local potential between the two sites; this prevents the logical qubits from undergoing any further rotation. Likewise, all on-site potentials μ_i are set to zero.

B. Matchgate representation

Now that we have obtained the single-qubit Hamiltonian required to effect arbitrary single-qubit gates, it is instructive to explore the underlying graph that yields the same set of matchgates. Following the discussion in Sec. II A, for a two-input, two-output gate one requires an underlying graph with at least six vertices. Consider therefore the six-vertex complete graph, with edges w_{ij} for all $i \neq j \in \{1, \dots, 6\}$. Suppose that the input and output vertices correspond to $\{1, 2\}$ and $\{4, 5\}$, respectively. Given external nodes $Z = \{1, 2, 4, 5\}$, the character matrix is given by

$$\chi(\Gamma, Z) = \begin{matrix} & \emptyset & 1 & 2 & 1,2 \\ \emptyset & \begin{pmatrix} a & b & c & d \\ e & f & g & h \\ i & j & k & \ell \\ m & n & o & p \end{pmatrix} \\ 4,5 & \end{matrix}. \qquad (32)$$

Let's work out the values of these 16 parameters. The simplest is

$$p = \chi(\Gamma, \{1, 2, 4, 5\}) = w_{36}. \qquad (33)$$

The next set of four can be evaluated under the assumption that vertex 6 is omittable:

$$h = \chi(\Gamma, \{1, 2, 4\}) = w_{35} = 0;$$
$$\ell = \chi(\Gamma, \{1, 2, 5\}) = w_{34} = 0;$$
$$n = \chi(\Gamma, \{1, 4, 5\}) = w_{23} = 0;$$
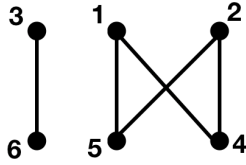$$o = \chi(\Gamma, \{2, 4, 5\}) = w_{13} = 0, \qquad (34)$$

FIG. 3. The matchgate graph representation of arbitrary single-qubit gates. The weights of the edges depend on the specific realization of the single-qubit operation.

where the zero values are imposed in order that the character matrix has the form of a matchgate. With these simplifications on the edge weights, it is straightforward to verify that $\chi(\Gamma, \{1\}) = \chi(\Gamma, \{2\}) = \chi(\Gamma, \{4\}) = \chi(\Gamma, \{5\}) = b = c = e = i = 0$. One may also readily obtain

$$d = \chi(\Gamma, \{1, 2\}) = w_{45}w_{36};$$
$$f = \chi(\Gamma, \{1, 5\}) = w_{24}w_{36};$$
$$j = \chi(\Gamma, \{1, 4\}) = -w_{25}w_{36};$$
$$g = \chi(\Gamma, \{2, 5\}) = -w_{14}w_{36};$$
$$k = \chi(\Gamma, \{2, 4\}) = w_{15}w_{36};$$
$$m = \chi(\Gamma, \{4, 5\}) = w_{12}w_{36}; \tag{35}$$

and

$$a = \chi(\Gamma, \emptyset) = (w_{12}w_{45} - w_{14}w_{25} + w_{15}w_{24})w_{36}. \tag{36}$$

Perhaps surprisingly, the graph underlying the matchgate is disconnected, with vertices 3 and 6 uncoupled from the remaining four vertices.

Comparing the matchgate expression (15) with the b_{ij} coefficients given by Eq. (29), one immediately obtains $w_{45} = w_{12} = 0$, and $w_{36} = e^{i(\mu_\ell + \mu_r)\tau/2}$. The underlying graph connectivity is depicted in Fig. 3. While general expressions for the remaining nonzero weights are a bit unwieldy, the values for the Z and X rotations, Eqs. (30) and (31), respectively, take simple forms. For the Z rotation, the remaining nonzero weights reduce to $w_{15} = e^{i\mu_r\tau}$ and $w_{24} = e^{i\mu_\ell\tau}$; the underlying graph therefore corresponds to three disconnected length-two paths. For the X rotation, the remaining nonzero weights reduce to $w_{14} = w_{25} = -ie^{i\mu_r\tau}\sin(t\tau)$ and $w_{24} = w_{15} = e^{i\mu_r\tau}\cos(t\tau)$.

C. Two-qubit entangling gates

Performing UQC also requires a two-qubit entangling gate. Within the current encoding, a general two-qubit quantum state is spanned by

$$|00\rangle_L = |10\rangle_1 \otimes |10\rangle_2, \; |01\rangle_L = |10\rangle_1 \otimes |01\rangle_2,$$
$$|10\rangle_L = |01\rangle_1 \otimes |10\rangle_2, \; |11\rangle_L = |01\rangle_1 \otimes |01\rangle_2, \tag{37}$$

where labelings 1 and 2 stand for logical qubits 1 and 2. Like the scheme in Ref. [2], the two-qubit gates are applied to the crossover sites, i.e., on sites r_1 and ℓ_2. On-site interactions are forbidden because of the Pauli principle, so that the shortest-range interactions possible correspond to nearest neighbors. Because all intersite tunneling is quenched, the only term in the Hamiltonian corresponds to the nearest-neighbor interaction:

$$H_{\text{int}} = \sum_i \lambda_{i,i+1} n_{r_i} n_{\ell_{i+1}}, \tag{38}$$

where $n_{r_i} = f_{r_i}^\dagger f_{r_i}$ is the number operator on the right site of qubit i; in principle, the interaction strength $\lambda_{i,i+1}$ can depend on the site indices. Evolution of qubits 1 and 2 under this Hamiltonian gives

$$e^{-iH_{\text{int}}\tau} = \begin{pmatrix} 1 & 0 & 0 & 0 \\ 0 & 1 & 0 & 0 \\ 0 & 0 & e^{-i\lambda_{12}\tau} & 0 \\ 0 & 0 & 0 & 1 \end{pmatrix} = \begin{pmatrix} 1 & 0 & 0 & 0 \\ 0 & 1 & 0 & 0 \\ 0 & 0 & -1 & 0 \\ 0 & 0 & 0 & 1 \end{pmatrix},$$
$$\tag{39}$$

if $\lambda_{12}\tau = \pi$. This is a nonmatchgate parity-preserving gate, equivalent to a CZ gate under local rotations.

D. Implementation with ultracold atomic gases

This approach to universal quantum computing requires the ability to generate double-well potentials, implement the initial conditions, dynamically adjust the tunneling amplitudes, apply local potentials, activate and deactivate nearest-neighbor interactions, and read out the atomic positions. All of these capabilities (among a host of others) are currently feasible in the context of ultracold atoms [19], which makes these systems particularly promising for the realization of universal quantum computing. While many other experimental approaches to quantum computation show promise, in this work we will focus on ultracold atomic environments as experimental applications of the proposed schemes.

One-dimensional double-well lattices result when polarized orthogonal optical standing waves controlled by electro-optical modulators are overlapped [20,21]. While the first applications of double-well potentials focused on bosons, fermions are now routinely cooled and trapped in optical lattices [22–24], including periodic [25,26] and double-well [27,28] lattices in one dimension. That said, this particular scheme is independent of the particle statistics as there is never an opportunity for the wave functions of two or more particles to overlap.

A key ingredient of the above scheme is the state preparation, where one spin-polarized fermion is loaded into each double well. This can be accomplished by cooling unpolarized interacting fermions in optical lattices, where they spontaneously form a Mott insulating state (i.e., with one fermion per site) characterized by antiferromagnetic spin correlations [17,28–31]. One spin component can then be preferentially ejected via a global resonant laser pulse [30–32]. The remaining atoms can be spin polarized using an external magnetic field, and the initial conditions can be obtained by cooling the fermions in the double-well lattice to its ground state. Alternatively, state preparation can be effected by manipulating atomic positions in initial random states using movable optical tweezers [33–37].

The manipulation of the site-to-site tunneling amplitudes, generation of local potentials, and the read-out can all be accomplished with the same technology of local addressing. Site-resolved microscopy originally employed a large numerical-aperture lens [38,39], and recent work has brought

the spatial resolution down to approximately half of the imaging laser wavelength this way [40]. More recently, techniques borrowed from super-resolution microscopy yielded spatial imaging resolution as small as 50 times smaller than the laser wavelength [41,42]. The read-out of the atomic positions has been successfully implemented in fermionic atoms such as ^{40}K [31,43,44] and ^{6}Li [17,28,30,45].

The last key ingredient is the inclusion of nearest-neighbor interactions on demand. Long-range interactions can be induced in ultracold atomic gases by promoting atoms to Rydberg states [46–49]. Because the interaction range falls off with distance d between atoms as d^{-6}, the Rydberg interactions can be chosen such that only nearest-neighboring atoms are affected. Another intriguing possibility is to induce dipole-dipole interactions via the application of external fields [50,51]. As on-demand interactions remain experimentally challenging in these systems, however, for the rest of this manuscript we consider the experimentally realizable Hubbard model, which requires on-site interactions that are native to ultracold atomic gases.

IV. SPIN-1/2 FERMIONS

After extending the matchgate formalism to spin-1/2 fermions by considering hopping between two sites, we show that the inclusion of on-site interactions in the Hubbard model breaks the matchgate paradigm. In one-dimensional systems, we show that it is impossible to implement a universal set of single-qubit gates if one assumes that hopping on the lattice is independent of spin, but that spin-dependent hopping promotes the matchgate circuits to UQC in the presence of on-site interactions assuming the ability to adjust the local hopping strengths and chemical potentials.

A. Extending matchgates to spin-1/2 fermions

The noninteracting Hamiltonian for spin-1/2 fermions on a lattice is

$$H_{\text{hop}} = -\sum_{\langle i,j\rangle,\sigma} (t_{ij\sigma} f_{i\sigma}^\dagger f_{j\sigma} + \text{H.c.}) - \sum_{i,\sigma} \mu_{i\sigma} n_{i\sigma}, \quad (40)$$

where $\langle ij \rangle$ denotes the inclusion of nearest neighbors only, and $n_{i\sigma} = f_{i\sigma}^\dagger f_{i\sigma}$ is the number operator for a fermion with spin $\sigma = \{\uparrow, \downarrow\}$ at site i. In general, the hopping amplitudes may depend on both position and spin, but hopping accompanied by spin flips is not included. In the two-site case where $i, j = \{1, 2\}$ only, at most four fermions can be accommodated. The number-preserving Hamiltonian is the 16-dimensional block-diagonal matrix,

$$H_{\text{hop}} = H_0 \oplus H_1 \oplus H_2 \oplus H_3 \oplus H_4, \quad (41)$$

where H_k corresponds to the k-particle block, with dimension $\binom{4}{k}$. If the evolution under this Hamiltonian can also be mapped to matchgates, one requires that

$$U_{\text{hop}} = e^{-iH_{\text{hop}}\tau} = G_\uparrow \otimes G_\downarrow, \quad (42)$$

where G_σ corresponds to the matchgate associated with spin σ. This is equivalent to showing that the Hamiltonian H_{hop} can be written as the Cartesian product,

$$H_{\text{hop}} = H_\uparrow \otimes I_\downarrow + I_\uparrow \otimes H_\downarrow, \quad (43)$$
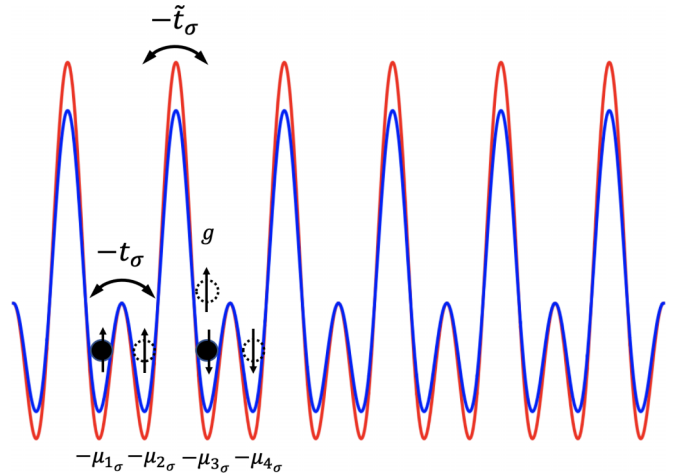
FIG. 4. The double-well lattice potential for spin-half fermions. Each successive double well contains at most one fermion with alternating spin projection. The spin-dependent hopping amplitudes are t_σ and $\tilde{t}_\sigma$ for intra- and interwell hopping, respectively. Local spin-dependent potentials are μ_{j_σ}, and on-site interactions are denoted by g.

which would imply

$$G_\uparrow = e^{-iH_\uparrow\tau}, \quad G_\downarrow = e^{-iH_\downarrow\tau}. \quad (44)$$

The proof that this is in fact the case is straightforward but unwieldy, and is therefore relegated to Appendix A.

The corresponding generator of the matchgate corresponds to two disconnected graphs, each of which is the graph depicted in Fig. 3. This is because two sets of spatially separated nodes and edges yields two independent matchgates (for different spin projections), which can be written as the form in Eq. (42). The presence of interactions between particles of opposite spin, discussed in detail below, gives rise to additional edges between these disconnected graphs. The resulting character matrix no longer will have the matchgate form.

B. The Hubbard model

The Hubbard model allows for on-site interactions, which can only occur if the fermions have a spin degree of freedom:

$$H = -\sum_{\langle ij\rangle,\sigma} (t_{ij\sigma} f_{i\sigma}^\dagger f_{j\sigma} + \text{H.c.}) - \sum_{i,\sigma} \mu_{i\sigma} n_{i\sigma}$$
$$+ g\sum_i n_{i\uparrow} n_{i\downarrow}, \quad (45)$$

where the parameter g represents the strength of on-site interactions between fermions of different spin projection. In the case where there are only two sites, the interaction term modifies the H_2, H_3, and H_4 blocks of the number-preserving Hamiltonian discussed above, in Sec. IV A. As shown in Appendix A, the presence of these terms violates the matchgate condition for all choices of interaction strength save $g = 0$. This suggests that the Hubbard model has the power to enable the fermions to effect arbitrary quantum gates.

In this work, we will consider only one-dimensional systems. Consider the double-well lattice depicted in Fig. 4,

inspired by the encoding scheme employed in Sec. III. The qubits are encoded as follows:

$$|0\rangle_1 = f_{1\uparrow}^\dagger|\emptyset\rangle; \quad |1\rangle_1 = f_{2\uparrow}^\dagger|\emptyset\rangle;$$
$$|0\rangle_2 = f_{3\downarrow}^\dagger|\emptyset\rangle; \quad |1\rangle_2 = f_{4\downarrow}^\dagger|\emptyset\rangle, \tag{46}$$

where the subscripts label the qubit index. The lattice is therefore one-quarter filled: sites 1 and 2 share one spin-up particle, and sites 3 and 4 share one spin-down particle, as depicted in Fig. 4. Like the spin-polarized case, high (but adjustable) potential barriers between double wells prevent hopping between different double wells unless demanded. The corresponding Hamiltonian can be written,

$$H = -\sum_{i,\sigma}(t_\sigma f_{2i-1\sigma}^\dagger f_{2i\sigma} + \tilde{t}_\sigma f_{2i\sigma}^\dagger f_{2i+1\sigma} + \text{H.c.})$$
$$- \sum_{i,\sigma}\mu_{i\sigma}n_{i\sigma} + g\sum_i n_{i\uparrow}n_{i\downarrow}, \tag{47}$$

where t_σ and $\tilde{t}_\sigma$ are the (potentially spin-dependent) hopping amplitudes within sites of a double well and between wells, respectively.

As each qubit is encoded by the presence or absence of a single fermion in a given double well, to perform single-qubit gates one can neglect hopping between adjacent double-well potentials and set $\tilde{t} = 0$. Under this condition, particles with different spin projection will never occupy the same site and the interaction term can also be neglected. Single-qubit gates are then implemented in precisely the same way for each separate double-well potential as in the spinless (spin-polarized) case treated in Sec. III A.

1. Spin-independent lattice

In order to utilize the on-site interaction to generate two-qubit gates, we must allow hopping of spin-up and spin-down fermions between adjacent double wells that were initially separated by the high potential barrier. The encoding of quantum information in the system could be disrupted if these two qubits fail to return to their previous positions; this is a key constraint that needs to be satisfied in the current scheme. As discussed in this subsection, this constraint is impossible

to satisfy under the assumption that the hopping between adjacent double wells is independent of spin.

The approach to generate an entangling gate between two nearest-neighbor fermionic qubits works as follows: Turn on the hopping between these two qubits for a certain amount of time, during which they pick up a phase and also return to where they start. Given the initial two-qubit state,

$$|\psi_0\rangle = (\alpha|1\uparrow\rangle + \beta|2\uparrow\rangle)(\gamma|3\downarrow\rangle + \delta|4\downarrow\rangle), \tag{48}$$

the goal is to produce the following state:

$$|\psi\rangle = \alpha\gamma|1\uparrow3\downarrow\rangle + \alpha\delta|1\uparrow4\downarrow\rangle + \beta\gamma e^{i\theta}|2\uparrow3\downarrow\rangle$$
$$+ \beta\delta|2\uparrow4\downarrow\rangle$$
$$= \alpha\gamma|00\rangle_L + \alpha\delta|01\rangle_L + \beta\gamma e^{i\theta}|10\rangle_L + \beta\delta|11\rangle_L, \tag{49}$$

where the two-qubit state becomes entangled as long as $\theta \neq 2\pi n$. In principle, the phase term could be located on any of the basis states, but the $|2\uparrow3\downarrow\rangle = |10\rangle_L$ is the most natural if hopping is induced between sites 2 and 3. With $\theta = \pi$, the entangling gate is equivalent to CZ under local unitaries, and could therefore also readily generate SWAP gates to induce entanglement between distant encoded qubits. For a spin-independent lattice, the hopping strengths in Eq. (47) are independent of spin, $\{t_\sigma, \tilde{t}_\sigma\} \to \{t, \tilde{t}\}$.

In the simplest model, intrawell hopping is turned off and the qubits' states are frozen by raising the barrier between sites 1 and 2, and between sites 3 and 4. Then hopping between sites 2 and 3 is enabled by lowering this potential barrier. As only states involved with sites 2 and 3 are affected, the target state and the Hamiltonian can be characterized by the number of particles on these sites:

$$|\psi\rangle = \underbrace{\alpha\gamma|1\uparrow3\downarrow\rangle}_{\text{one-body}} + \underbrace{\alpha\delta|1\uparrow4\downarrow\rangle}_{\text{vacuum}} + \underbrace{\beta\gamma|2\uparrow3\downarrow\rangle}_{\textbf{two-body}}$$
$$+ \underbrace{\beta\delta|2\uparrow4\downarrow\rangle}_{\text{one-body}}, \tag{50}$$

and

$$H = H_{0\text{b}} \oplus H_{1\text{b}} \oplus H_{2\text{b}}, \tag{51}$$

where the submatrices have labels nb which stand for "number of bodies" and are given by

$$H_{0\text{b}} = (0);$$

$$H_{1\text{b}} = \begin{pmatrix} -\mu_2 & -\tilde{t} & 0 & 0 \\ -\tilde{t} & -\mu_3 & 0 & 0 \\ 0 & 0 & -\mu_2 & -\tilde{t} \\ 0 & 0 & -\tilde{t} & -\mu_3 \end{pmatrix} \begin{matrix} |2\uparrow\rangle \\ |3\uparrow\rangle \\ |2\downarrow\rangle \\ |3\downarrow\rangle \end{matrix},$$

$$H_{2\text{b}} = \begin{pmatrix} -2\mu_2 + g & -\tilde{t} & -\tilde{t} & 0 \\ -\tilde{t} & -\mu_2 - \mu_3 & 0 & -\tilde{t} \\ -\tilde{t} & 0 & -\mu_2 - \mu_3 & -\tilde{t} \\ 0 & -\tilde{t} & -\tilde{t} & -2\mu_3 + g \end{pmatrix} \begin{matrix} |2\uparrow2\downarrow\rangle \\ |2\uparrow3\downarrow\rangle \\ |3\uparrow2\downarrow\rangle \\ |3\uparrow3\downarrow\rangle \end{matrix}, \tag{52}$$

where $\tilde{t} = \tilde{t}_{23} = \tilde{t}_{32}$ is the hopping amplitude for both spin-up and down fermions at sites 2 and 3. The states are shown explicitly for convenience.

The input quantum state (50) requires that the time evolution apply the identity to the zero and one-body matrices but a nontrivial phase to the two-body term. Because the

two submatrices in H_{1b} are exactly the same, one only need consider one 2×2 matrix. Choosing $\tilde{t}$ as the energy scale, the time evolution of the one-body term becomes

$$U_{1b} = \exp \left[i \begin{pmatrix} \tilde{\mu}_2 & 1 \\ 1 & \tilde{\mu}_3 \end{pmatrix} \tilde{\tau} \right], \qquad (53)$$

where $\tilde{\mu}_i = \mu_i/\tilde{t}$ and $\tilde{\tau} = \tau/\tilde{t}$. With the restriction that the (1,1) and (4,4) matrix elements of U_{1b} must have unit norm, one obtains

$$U_{1b} = (-1)^n \exp \left[-in\pi \frac{\tilde{\mu}_2 + \tilde{\mu}_3}{\sqrt{4 + (\tilde{\mu}_2 - \tilde{\mu}_3)^2}} \right] I \qquad (54)$$

for $\tilde{\tau} = 2\pi n/\sqrt{4 + (\tilde{\mu}_2 - \tilde{\mu}_3)^2}$. For $n = 1$, the condition that $U_{1b} = I$ requires $\tilde{\mu}_3 = 1/\tilde{\mu}_2$, while $n = 2$ yields $\tilde{\mu}_3 = -\tilde{\mu}_2$; larger values of n yield more complicated (but not very insightful) expressions for $\tilde{\mu}_3$ in terms of n and $\tilde{\mu}_2$.

This leaves two adjustable parameters ($\tilde{g} = g/\tilde{t}$ and $\tilde{\mu}_2$) in H_{2b}. One need only consider the (2,2) element of the unitary $U_{2b} = \exp(-iH_{2b}\tau)$, as no other two-body states appear in Eq. (50). After evolution time $\tilde{\tau}$ this element must have both a nontrivial phase and unit norm to ensure that none of the quantum information has leaked to a noncoding space. The analytics are unwieldy, so we present instead a numerical analysis for specific choices of $\tilde{g}$ and $\tilde{\mu}_2$ for the specific case $\tilde{\mu}_3 = 1/\tilde{\mu}_2$. The numerical results can be found in Table I in Appendix B. It is clear that the only case where the (2,2) matrix element has unit norm corresponds to $\tilde{g} = 0$ and therefore zero phase: no entanglement can be generated in the absence of particle interactions. For the case $\tilde{\mu}_3 = -\tilde{\mu}_2$, there is again no nonzero value of $\tilde{g}$ for which the (2,2) norm is unitary with a nontrivial phase. Perhaps surprisingly, a nontrivial interaction strength $\tilde{g} = 3$ nevertheless yields $U_{2b} = I$ for $\tilde{\mu}_2 = \tilde{\mu}_3 = 0$ and an evolution time of $\tilde{\tau} = 2\pi$.

The restriction of zero phases on both one-body terms is perhaps too strong. One can instead suppose that accumulated phases on these terms could work with the two-body term to nevertheless yield an entangling gate while preserving the unit norms on the diagonals of the one-body unitaries. Keeping these phases, we also numerically analyze U_{2b} (using the appropriate relationships between μ_2 and μ_3). Unfortunately, the same conclusion is reached as above: No nonzero value of g can yield an entangling gate. This failure is readily explained; on-site phases from one-body terms can be generated only by controlling the local potentials at sites 2 and 3, which clearly has no power to entangle qubits because entanglement is impervious to local operations.

In light of the fact that local potentials fail to generate entanglement, a full analytical calculation can be obtained without loss of generality by considering only the $\tilde{\mu}_2 = \tilde{\mu}_3 = 0$ case. The minimum evolution time is then $\tilde{\tau} = \pi$, and the (2,2) element of U_{2b} becomes

$$U_{2b}(2,2) = \frac{e^{-\frac{i}{2}(\tilde{g}+\sqrt{16+\tilde{g}^2})\pi}}{4\sqrt{16 + \tilde{g}^2}} \Big[(-1 + e^{i\sqrt{16+\tilde{g}^2}\pi})\tilde{g} \\ + (1 + e^{i\sqrt{16+\tilde{g}^2}\pi} + 2e^{\frac{i}{2}(\tilde{g}+\sqrt{16+\tilde{g}^2})\pi})\sqrt{16 + \tilde{g}^2} \Big]. \qquad (55)$$

The goal is to make this entry a phase; this is true only when the following criteria are satisfied:

$$e^{i\sqrt{16+g^2}\pi} = 1, \quad e^{\frac{i}{2}(g+\sqrt{16+g^2})\pi} = 1. \qquad (56)$$

Unfortunately, the resulting phase $e^{-\frac{i}{2}(g+\sqrt{16+g^2})\pi} = 1$. This agrees with the numerical calculation discussed above. These two equations can be solved for the on-site interaction g:

$$\tfrac{1}{2}(\tilde{g} + \sqrt{16 + \tilde{g}^2}) = 2m, \quad \sqrt{16 + \tilde{g}^2} = 2n, \quad m, n \in \mathbb{Z}. \qquad (57)$$

Thus, the on-site interaction is found to be $\tilde{g} = 4m - 2n$, where the integers m, n satisfy $n = m + \frac{1}{m}$. The only solution here is that $m = 1, n = 2$, which gives us $g = 0$. Again, this analytical result agrees with the numerical result in Appendix B.

Thus far, the analysis has been restricted to hopping between sites 2 and 3. It is reasonable to test the effect of adding hopping between sites 1 and 2 (or its symmetric counterpart sites 3 and 4) to check if this helps in generating entanglement. In this case, the general quantum state becomes

$$|\psi\rangle = \underbrace{\alpha\gamma|1{\uparrow}3{\downarrow}\rangle}_{\textbf{two-body}} + \underbrace{\alpha\delta|1{\uparrow}4{\downarrow}\rangle}_{\text{one-body}} + \underbrace{\beta\gamma|2{\uparrow}3{\downarrow}\rangle}_{\textbf{two-body}} \\ + \underbrace{\beta\delta|2{\uparrow}4{\downarrow}\rangle}_{\text{one-body}}, \qquad (58)$$

which is the same as the state (50), but now the fermion occupation has changed. Unfortunately, as fermionic hopping is a local operation that maps to matchgates, adding new hopping cannot generate any entanglement.

2. Spin-dependent lattice for two-qubit gates

Given the failure of a spin-independent Hubbard Hamiltonian to generate entanglement, consider now a spin-dependent lattice model. In this case, the matrices become $H_{0b} = (0)$ and

$$H_{1b} = \begin{pmatrix} -\mu_{2\uparrow} & -\tilde{t}_\uparrow & 0 & 0 \\ -\tilde{t}_\uparrow & -\mu_{3\uparrow} & 0 & 0 \\ 0 & 0 & -\mu_{2\downarrow} & -\tilde{t}_\downarrow \\ 0 & 0 & -\tilde{t}_\downarrow & -\mu_{3\downarrow} \end{pmatrix}; \quad H_{2b} = \begin{pmatrix} -\mu_{2\uparrow} - \mu_{2\downarrow} + g & -\tilde{t}_\downarrow & -\tilde{t}_\uparrow & 0 \\ -\tilde{t}_\downarrow & -\mu_{2\uparrow} - \mu_{3\downarrow} & 0 & -\tilde{t}_\uparrow \\ -\tilde{t}_\uparrow & 0 & -\mu_{2\downarrow} - \mu_{3\uparrow} & -\tilde{t}_\downarrow \\ 0 & -\tilde{t}_\uparrow & -\tilde{t}_\downarrow & -\mu_{3\uparrow} - \mu_{3\downarrow} + g \end{pmatrix}. \qquad (59)$$

Because the hopping strengths between sites 2 and 3 and the local potentials at sites 2 and 3 can be controlled separately for spins $\uparrow$ and $\downarrow$ by assumption, consider the simplest nontrivial

configuration of parameters:

$$\tilde{t}_\uparrow = \mu_{2\uparrow} = \mu_{2\downarrow} = \mu_{3\uparrow} = \mu_{3\downarrow} = 0. \qquad (60)$$

This choice implies zero hopping for spin $\uparrow$ and no local potentials, keeping only hopping for spin $\downarrow$ and the on-site interaction g. The one-body terms impose the constraint $\tilde{\tau} = 2\pi n/\tilde{t}_\downarrow$, $n \in \mathbb{Z}$. Again enforcing unit norm on the (2,2) matrix element of the two-body unitary, one obtains $g = \sqrt{m^2 - 4n\tilde{t}_\downarrow}/n$, $|m| \geqslant 2|n|$, or a phase of $(-1)^m e^{\pm i\pi\sqrt{m^2 - 4n^2}}$. This is a nontrivial phase, and therefore entanglement is possible for a spin-dependent lattice.

Ideally, for a (local-unitary equivalent) CZ gate, one would like $m \pm \sqrt{m^2 - 4n^2} = 2k + 1$ to hold. Unfortunately, this is impossible; expanding the two sides of this equation and rearranging them, one obtains

$$4km + 2m - 4k - 1 \overset{?}{=} 4n^2 + 4k^2. \tag{61}$$

Unfortunately, this equality can never be satisfied as the left side is always odd while the right side is even. That said, with a judicious parameter set it is possible to achieve a phase that is arbitrarily close to an odd multiple of π. For example, $\{n, m\} = \{6, 72\}$ gives a phase of approximately 142.993π, or a coefficient of $-0.9998 + 0.0221i$. These choices require the physical parameters $\tau = 12\pi/\tilde{t}_\downarrow$ and $g \approx 11.83\tilde{t}_\downarrow$. More accurate approximations to the phase would require longer evolution times.

Because entanglement can already be generated in the spin-dependent lattice with minimal parameters, it is conceivable that the addition of local potentials can change the value of the phase. While local potentials cannot produce entanglement on their own if interactions are unable to do so, in principle local potentials could change the magnitude of entanglement generated by interactions. Consider instead the following parameters:

$$\tilde{t}_\uparrow = \mu_{2\uparrow} = \mu_{3\uparrow} = \mu_{3\downarrow} = 0, \tag{62}$$

while $\mu_{2\downarrow} \neq 0$. Choosing $\tilde{t}_\downarrow$ as the energy scale, the requirement that the (3,3) and (4,4) matrix elements of the one-body unitary have unit norm yields the condition,

$$\frac{\tilde{\tau}}{2}\sqrt{\tilde{\mu}_{2\downarrow}^2 + 4} = 2k\pi, \ k \in \mathbb{N}. \tag{63}$$

Thus, setting

$$\tilde{\tau} = \frac{4k\pi}{\sqrt{\tilde{\mu}_{2\downarrow}^2 + 4}} \tag{64}$$

gives $U_{1b} = I \oplus e^{i2\pi k\tilde{\mu}_{2\downarrow}/\sqrt{4+\tilde{\mu}_{2\downarrow}^2}}I$.

Next consider the two-particle unitary. The relevant (2,2) matrix element can be made a pure phase term,

$$U_{2b}(2,2) = e^{i2\pi k\tilde{\mu}_{2\downarrow}/\sqrt{4+\tilde{\mu}_{2\downarrow}^2}}(-1)^n e^{-i2\pi k\tilde{g}/\sqrt{4+\tilde{\mu}_{2\downarrow}^2}}, \tag{65}$$

if

$$\frac{2\pi k\sqrt{4 + (\tilde{g} - \tilde{\mu}_{2\downarrow})^2}}{\sqrt{4 + \tilde{\mu}_{2\downarrow}^2}} = \pi n, \ n \in \mathbb{N}. \tag{66}$$

Note that the first term in Eq. (65) is the same as the one-body term. For the remaining terms to equal negative unity (with an

eye on producing a gate equivalent to a CZ), one can choose

$$\tilde{g} = \frac{(n-1)\sqrt{4 + \tilde{\mu}_{2\downarrow}^2}}{2k}. \tag{67}$$

The state then becomes

$$|\psi\rangle = e^{i2\pi k\tilde{\mu}_{2\downarrow}/\sqrt{4+\tilde{\mu}_{2\downarrow}^2}}\alpha\gamma|1{\uparrow}3{\downarrow}\rangle + \alpha\delta|1{\uparrow}4{\downarrow}\rangle$$
$$- e^{i2\pi k\tilde{\mu}_{2\downarrow}/\sqrt{4+\tilde{\mu}_{2\downarrow}^2}}\beta\gamma|2{\uparrow}3{\downarrow}\rangle + \beta\delta|2{\uparrow}4{\downarrow}\rangle. \tag{68}$$

Inserting the expression for the interaction strength, Eq. (67), into Eq. (66) allows for the determination of the local potential:

$$\tilde{\mu}_{2\downarrow} = \pm\frac{2(2n - 1 - 4k^2)}{\sqrt{(4k^2 - 1)[(2n-1)^2 - 4k^2]}}, \tag{69}$$

which requires $n > k$. In turn this yields the interaction strength:

$$\tilde{g} = \frac{4(n-1)^2}{\sqrt{(4k^2 - 1)[(2n-1)^2 - 4k^2]}}. \tag{70}$$

Finally, the state becomes

$$|\psi\rangle = e^{\pm i\pi(2n-1-4k^2)/2(n-1)}\alpha\gamma|1{\uparrow}3{\downarrow}\rangle + \alpha\delta|1{\uparrow}4{\downarrow}\rangle$$
$$- e^{\pm i\pi(2n-1-4k^2)/2(n-1)}\beta\gamma|2{\uparrow}3{\downarrow}\rangle + \beta\delta|2{\uparrow}4{\downarrow}\rangle$$
$$= i\alpha\gamma|1{\uparrow}3{\downarrow}\rangle + \alpha\delta|1{\uparrow}4{\downarrow}\rangle - i\beta\gamma|2{\uparrow}3{\downarrow}\rangle$$
$$+ \beta\delta|2{\uparrow}4{\downarrow}\rangle \tag{71}$$

for the simple case $k = 1$ and $n = 2$ and $\tilde{\mu}_{2\downarrow} > 0$; one also obtains the parameters $\tilde{\mu}_{2\downarrow} = 2/\sqrt{15}$, $\tilde{g} = 4/\sqrt{15}$, and $\tilde{\tau} = \sqrt{15}\pi/2$.

The additional factors of i in the expression for the state, Eq. (71), can be eliminated by noticing that they are common to states with spin-down on site 3. Turning off all hopping and adding only a local potential $\tilde{\mu}_{3\downarrow}$ yields an additional phase of $e^{-i\tilde{\mu}_{3\downarrow}\tilde{\tau}'}$ on all states with support on site 3. Setting $\tilde{\tau}' = 3\pi/2\tilde{\mu}_{3\downarrow}$ cancels all unwanted phases, and one is left with the state,

$$|\psi\rangle = \alpha\gamma|1{\uparrow}3{\downarrow}\rangle + \alpha\delta|1{\uparrow}4{\downarrow}\rangle - \beta\gamma|2{\uparrow}3{\downarrow}\rangle$$
$$+ \beta\delta|2{\uparrow}4{\downarrow}\rangle, \tag{72}$$

where a CZ gate (modulo local unitaries) has been performed.

This scheme hinges on the ability to allow one spin component to hop while preventing the other component from doing so. In fact, such spin-dependent hopping has been realized in ultracold atomic gases [52,53]. Together with the technology discussed in detail in Sec. III D, these systems provide all of the requirements to perform universal quantum gates.

V. CONCLUSIONS

Through the investigation of Hamiltonians that are within the family of (fermionic) Hubbard models, a universal set of quantum gates can be generated making use of a specially prepared one-dimensional lattice. In the spinless case, the standard matchgates are elevated to a universal gate set via

the interaction of fermions on nearest-neighbor sites. In the spin-1/2 case, the single-qubit gates fall under an extension of the set of matchgates, where the logical qubits are encoded in the odd-parity subspace. These generalized matchgates are promoted to universality via the physical interaction beween fermions of opposite spin on a single lattice site, but controlled-PHASE gates are realizable only if the hopping strength can depend on the spin projection. Implementations for both the spinless and spin-1/2 cases are suggested in the context of ultracold atoms in optical lattices and optical trap arrays.

APPENDIX A: NONINTERACTING SPIN-1/2 FERMIONS YIELD MATCHGATES

Consider the specific form of $H_\uparrow \otimes I_\downarrow$ and $I_\uparrow \otimes H_\downarrow$ for spin-1/2 fermions hopping between two sites:

$$H_\uparrow \otimes I_\downarrow = \begin{pmatrix} 0 & 0 & 0 & 0 \\ 0 & -\mu_{1\uparrow} & -t_{1\uparrow 2\uparrow} & 0 \\ 0 & -t_{2\uparrow 1\uparrow} & -\mu_{2\uparrow} & 0 \\ 0 & 0 & 0 & -\mu_{1\uparrow}-\mu_{2\uparrow} \end{pmatrix} \otimes \begin{pmatrix} 1 & 0 & 0 & 0 \\ 0 & 1 & 0 & 0 \\ 0 & 0 & 1 & 0 \\ 0 & 0 & 0 & 1 \end{pmatrix}, \tag{A1}$$

and

$$I_\uparrow \otimes H_\downarrow = \begin{pmatrix} 1 & 0 & 0 & 0 \\ 0 & 1 & 0 & 0 \\ 0 & 0 & 1 & 0 \\ 0 & 0 & 0 & 1 \end{pmatrix} \otimes \begin{pmatrix} 0 & 0 & 0 & 0 \\ 0 & -\mu_{1\downarrow} & -t_{1\downarrow 2\downarrow} & 0 \\ 0 & -t_{2\downarrow 1\downarrow} & -\mu_{2\downarrow} & 0 \\ 0 & 0 & 0 & -\mu_{1\downarrow}-\mu_{2\downarrow} \end{pmatrix}. \tag{A2}$$

The hopping Hamiltonian $H_{\text{hop}} = H_\uparrow \otimes I_\downarrow + I_\uparrow \otimes H_\downarrow$ then becomes

$$H_{\text{hop}} = - \left(\begin{array}{cccccccc}
0 & 0 & 0 & 0 & 0 & 0 & 0 & 0 & 0 \\
0 & \mu_{1\downarrow} & t_\downarrow & 0 & 0 & 0 & 0 & 0 & 0 & 0 \\
0 & t_\downarrow & \mu_{2\downarrow} & 0 & 0 & 0 & 0 & 0 & 0 & 0 \\
0 & 0 & 0 & \mu_{1\downarrow}+\mu_{2\downarrow} & 0 & 0 & 0 & 0 & 0 & 0 \\
0 & 0 & 0 & 0 & \mu_{1\uparrow} & 0 & 0 & 0 & t_\uparrow & 0 \\
0 & 0 & 0 & 0 & 0 & \mu_{1\downarrow}+\mu_{1\uparrow} & t_\downarrow & 0 & 0 & t_\uparrow \\
0 & 0 & 0 & 0 & 0 & t_\downarrow & \mu_{1\uparrow}+\mu_{2\downarrow} & 0 & 0 & 0 \\
0 & 0 & 0 & 0 & 0 & 0 & 0 & \mu_{1\downarrow}+\mu_{2\downarrow}+\mu_{1\uparrow} & 0 & 0 \\
0 & 0 & 0 & 0 & t_\uparrow & 0 & 0 & 0 & \mu_{2\uparrow} & 0 \\
0 & 0 & 0 & 0 & 0 & t_\uparrow & 0 & 0 & 0 & \mu_{1\downarrow}+\mu_{2\uparrow} \\
0 & 0 & 0 & 0 & 0 & 0 & t_\uparrow & 0 & 0 & t_\downarrow \\
0 & 0 & 0 & 0 & 0 & 0 & 0 & t_\uparrow & 0 & 0 \\
0 & 0 & 0 & 0 & 0 & 0 & 0 & 0 & 0 & 0 \\
0 & 0 & 0 & 0 & 0 & 0 & 0 & 0 & 0 & 0 \\
0 & 0 & 0 & 0 & 0 & 0 & 0 & 0 & 0 & 0 \\
0 & 0 & 0 & 0 & 0 & 0 & 0 & 0 & 0 & 0 \\
\end{array} \right. \cdots$$

$$\left. \begin{array}{cccccc}
0 & 0 & 0 & 0 & 0 & 0 \\
0 & 0 & 0 & 0 & 0 & 0 \\
0 & 0 & 0 & 0 & 0 & 0 \\
0 & 0 & 0 & 0 & 0 & 0 \\
0 & 0 & 0 & 0 & 0 & 0 \\
0 & 0 & 0 & 0 & 0 & 0 \\
t_\uparrow & 0 & 0 & 0 & 0 & 0 \\
0 & t_\uparrow & 0 & 0 & 0 & 0 \\
0 & 0 & 0 & 0 & 0 & 0 \\
t_\downarrow & 0 & 0 & 0 & 0 & 0 \\
\mu_{2\downarrow}+\mu_{2\uparrow} & 0 & 0 & 0 & 0 & 0 \\
0 & \mu_{1\downarrow}+\mu_{2\downarrow}+\mu_{2\uparrow} & 0 & 0 & 0 & 0 \\
0 & 0 & \mu_{1\uparrow}+\mu_{2\uparrow} & 0 & 0 & 0 \\
0 & 0 & 0 & \mu_{1\downarrow}+\mu_{1\uparrow}+\mu_{2\uparrow} & t_\downarrow & 0 \\
0 & 0 & 0 & t_\downarrow & \mu_{2\downarrow}+\mu_{1\uparrow}+\mu_{2\uparrow} & 0 \\
0 & 0 & 0 & 0 & 0 & \mu_{1\downarrow}+\mu_{2\downarrow}+\mu_{1\uparrow}+\mu_{2\uparrow}
\end{array} \right)$$

$$
= -(0) \oplus \begin{pmatrix} \mu_{1\downarrow} & t_\downarrow \\ t_\downarrow & \mu_{2\downarrow} \end{pmatrix} \oplus \begin{pmatrix} \mu_{1\uparrow} & t_\uparrow \\ t_\uparrow & \mu_{2\uparrow} \end{pmatrix} \oplus (\mu_{1\downarrow} + \mu_{2\downarrow}) \oplus \begin{pmatrix} \mu_{1\downarrow} + \mu_{1\uparrow} & t_\downarrow & t_\uparrow & 0 \\ t_\downarrow & \mu_{1\uparrow} + \mu_{2\downarrow} & 0 & t_\uparrow \\ t_\uparrow & 0 & \mu_{1\downarrow} + \mu_{2\uparrow} & t_\downarrow \\ 0 & t_\uparrow & t_\downarrow & \mu_{2\downarrow} + \mu_{2\uparrow} \end{pmatrix}
$$

$$
\oplus (\mu_{1\uparrow} + \mu_{2\uparrow}) \oplus \begin{pmatrix} \mu_{1\downarrow} + \mu_{2\downarrow} + \mu_{1\uparrow} & t_\uparrow \\ t_\uparrow & \mu_{1\downarrow} + \mu_{2\downarrow} + \mu_{2\uparrow} \end{pmatrix} \oplus \begin{pmatrix} \mu_{1\downarrow} + \mu_{1\uparrow} + \mu_{2\uparrow} & t_\downarrow \\ t_\downarrow & \mu_{2\downarrow} + \mu_{1\uparrow} + \mu_{2\uparrow} \end{pmatrix}
$$

$$
\oplus (\mu_{1\downarrow} + \mu_{2\downarrow} + \mu_{1\uparrow} + \mu_{2\uparrow}), \tag{A3}
$$

where the last expression follows from row and column permutations. It is clear that this corresponds exactly to the block-diagonal representation of the k-particle Hamiltonian,

$$
H = (-t_\uparrow c_{2\uparrow}^\dagger c_{1\uparrow} - t_\downarrow c_{2\downarrow}^\dagger c_{1\downarrow} + \text{H.c.}) - \mu_\uparrow (n_{1\uparrow} + n_{2\uparrow}) - \mu_\downarrow (n_{1\downarrow} + n_{2\downarrow}), \tag{A4}
$$

for $0 \leqslant k \leqslant 4$, assuming that basis states are defined as $|n_{1\uparrow} n_{2\uparrow} n_{1\downarrow} n_{2\downarrow}\rangle$ with $n_{i\sigma} \in \{0, 1\}$. Note that the k-particle blocks themselves decompose into $\{1, 2, 3, 2, 1\}$ smaller blocks for $k = 0, \ldots, 4$.

In the presence of on-site interactions, the two-particle Hamiltonian,

$$
H = (-t_\uparrow c_{2\uparrow}^\dagger c_{1\uparrow} - t_\downarrow c_{2\downarrow}^\dagger c_{1\downarrow} + \text{H.c.}) - \mu_\uparrow (n_{1\uparrow} + n_{2\uparrow}) - \mu_\downarrow (n_{1\downarrow} + n_{2\downarrow}) + g(n_{1\downarrow} n_{1\uparrow} + n_{2\downarrow} n_{2\uparrow}), \tag{A5}
$$

takes the block-diagonal form:

$$
H_{\text{tot}} = -(0) \oplus \begin{pmatrix} \mu_{1\downarrow} & t_\downarrow \\ t_\downarrow & \mu_{2\downarrow} \end{pmatrix} \oplus \begin{pmatrix} \mu_{1\uparrow} & t_\uparrow \\ t_\uparrow & \mu_{2\uparrow} \end{pmatrix} \oplus (\mu_{1\downarrow} + \mu_{2\downarrow}) \oplus \begin{pmatrix} g + \mu_{1\downarrow} + \mu_{1\uparrow} & t_\downarrow & t_\uparrow & 0 \\ t_\downarrow & \mu_{1\uparrow} + \mu_{2\downarrow} & 0 & t_\uparrow \\ t_\uparrow & 0 & \mu_{1\downarrow} + \mu_{2\uparrow} & t_\downarrow \\ 0 & t_\uparrow & t_\downarrow & g + \mu_{2\downarrow} + \mu_{2\uparrow} \end{pmatrix}
$$

$$
\oplus (\mu_{1\uparrow} + \mu_{2\uparrow}) \oplus \begin{pmatrix} g + \mu_{1\downarrow} + \mu_{2\downarrow} + \mu_{1\uparrow} & t_\uparrow \\ t_\uparrow & g + \mu_{1\downarrow} + \mu_{2\downarrow} + \mu_{2\uparrow} \end{pmatrix} \oplus \begin{pmatrix} g + \mu_{1\downarrow} + \mu_{1\uparrow} + \mu_{2\uparrow} & t_\downarrow \\ t_\downarrow & g + \mu_{2\downarrow} + \mu_{1\uparrow} + \mu_{2\uparrow} \end{pmatrix}
$$

$$
\oplus (2g + \mu_{1\downarrow} + \mu_{2\downarrow} + \mu_{1\uparrow} + \mu_{2\uparrow}). \tag{A6}
$$

Assuming the interacting Hamiltonian has the matchgate form, the total Hamiltonian must be able to be expressed as $H_{\text{tot}} = H_\uparrow' \otimes I_\downarrow + I_\uparrow \otimes H_\downarrow'$, where

$$
H_\sigma' = \begin{pmatrix} 0 & 0 & 0 & 0 \\ 0 & k_{1\sigma} & k_{2\sigma} & 0 \\ 0 & k_{2\sigma} & k_{3\sigma} & 0 \\ 0 & 0 & 0 & k_{1\sigma} + k_{3\sigma} \end{pmatrix}, \tag{A7}
$$

where $\sigma \in \{\uparrow, \downarrow\}$ and $k_{i\sigma}$ are arbitrary parameters. Comparison with Eq. (A6) implies that $k_{i\sigma} = g + \mu_{i\sigma}$ and simultaneously $k_{i\sigma} = \mu_{i\sigma}$ for $i = 1, 2$, which is possible only if $g = 0$. That said, the matchgate criterion is less restrictive, requiring only that $e^{-iH_{\text{tot}}\tau} = G_\uparrow' \otimes G_\downarrow'$ for some choice of parameters

g and t. The last block in Eq. (A6) imposes the constraint $2g\tau = 2\pi n$, while the second-to-last and third-to-last blocks impose $g\tau = 2\pi m$, with integer m, n; the second condition evidently supersedes the first, so that $g = 2\pi m/\tau$. It remains only to determine if there exist specific values of τ for which the exponentiation of the fifth block in Eq. (A6) yields the same matrix as when $g = 0$, and it is straightforward to verify that this is not possible for any choice of the remaining parameters.

APPENDIX B: NUMERICAL RESULTS FOR THE HUBBARD MODEL WITH SPIN-INDEPENDENT HOPPING

TABLE I. The phase and norm of the two-body term $|2\uparrow 3\downarrow\rangle$ in Eq. (50), not including the state-dependent $\beta\gamma$ contribution, for spin-half fermions in the Hubbard model with spin-independent hopping.

$\tilde{\mu}_2$	$\tilde{g}$	Density	Phase(π)	$\tilde{\mu}_2$	$\tilde{g}$	Density	Phase(π)	$\tilde{\mu}_2$	$\tilde{g}$	Density	Phase(π)
0.1	−1.0	0.993012	0.00745759	0.4	−0.2	0.980642	0.0421786	0.7	0.6	0.73859	−0.163649
0.1	−0.8	0.995521	0.00598884	**0.4**	**0.0**	**1.0**	**0.0**	0.7	0.8	0.577803	−0.212813
0.1	−0.6	0.997477	0.00450487	0.4	0.2	0.980642	−0.0421786	0.8	−1.0	0.460391	0.245466
0.1	−0.4	0.998878	0.00300953	0.4	0.4	0.924252	−0.0842184	0.8	−0.8	0.614348	0.20292
0.1	−0.2	0.999719	0.00150665	0.4	0.6	0.835698	−0.125969	0.8	−0.6	0.76334	0.155565
0.1	**0.0**	**1.0**	**0.0**	0.4	0.8	0.722508	−0.167257	0.8	−0.4	0.888006	0.10518
0.1	0.2	0.999719	−0.00150665	0.4	1.0	0.59407	−0.20786	0.8	−0.2	0.970922	0.0530067

TABLE I. (*Continued*).

$\tilde{\mu}_2$	$\tilde{g}$	Density	Phase(π)	$\tilde{\mu}_2$	$\tilde{g}$	Density	Phase(π)	$\tilde{\mu}_2$	$\tilde{g}$	Density	Phase(π)
0.1	0.4	0.998878	−0.00300953	0.5	−1.0	0.465361	0.258526	**0.8**	**0.0**	**1.0**	**0.0**
0.1	0.6	0.997477	−0.00450487	0.5	−0.8	0.622976	0.209325	0.8	0.2	0.970922	−0.0530067
0.1	0.8	0.995521	−0.00598884	0.5	−0.6	0.771225	0.158276	0.8	0.4	0.888006	−0.10518
0.1	1.0	0.993012	−0.00745759	0.5	−0.4	0.892651	0.106076	0.8	0.6	0.76334	−0.155565
0.2	−1.0	0.921425	0.0494269	0.5	−0.2	0.972273	0.0531965	0.8	0.8	0.614348	−0.20292
0.2	−0.8	0.949163	0.039883	**0.5**	**0.0**	**1.0**	**0.0**	0.8	1.0	0.460391	−0.245466
0.2	−0.6	0.971164	0.0301065	0.5	0.2	0.972273	−0.0531965	0.9	−1.0	0.500339	0.240856
0.2	−0.4	0.987107	0.0201618	0.5	0.4	0.892651	−0.106076	0.9	−0.8	0.648705	0.196998
0.2	−0.2	0.996765	0.0101078	0.5	0.6	0.771225	−0.158276	0.9	−0.6	0.787354	0.149939
0.2	**0.0**	**1.0**	**0.0**	0.5	0.8	0.622976	−0.209325	0.9	−0.4	0.900398	0.100902
0.2	0.2	0.996765	−0.0101078	0.5	1.0	0.465361	−0.258526	0.9	−0.2	0.974303	0.050716
0.2	0.4	0.987107	−0.0201618	0.6	−1.0	0.406373	0.267638	**0.9**	**0.0**	**1.0**	**0.0**
0.2	0.6	0.971164	−0.0301065	0.6	−0.8	0.572701	0.220232	0.9	0.2	0.974303	−0.050716
0.2	0.8	0.949163	−0.039883	0.6	−0.6	0.736422	0.168184	0.9	0.4	0.900398	−0.100902
0.2	1.0	0.921425	−0.0494269	0.6	−0.4	0.874832	0.113396	0.9	0.6	0.787354	−0.149939
0.3	−1.0	0.764985	0.126308	0.6	−0.2	0.967436	0.0570528	0.9	0.8	0.648705	−0.196998
0.3	−0.8	0.844452	0.101833	**0.6**	**0.0**	**1.0**	**0.0**	0.9	1.0	0.500339	−0.240856
0.3	−0.6	0.910196	0.0768075	0.6	0.2	0.967436	−0.0570528	1.0	−1.0	0.514615	0.239762
0.3	−0.4	0.959339	0.0514022	0.6	0.4	0.874832	−0.113396	1.0	−0.8	0.661186	0.195256
0.3	−0.2	0.989721	0.0257586	0.6	0.6	0.736422	−0.168184	1.0	−0.6	0.796175	0.148144
0.3	**0.0**	**1.0**	**0.0**	0.6	0.8	0.572701	−0.220232	1.0	−0.4	0.904983	0.0994785
0.3	0.2	0.989721	−0.0257586	0.6	1.0	0.406373	−0.267638	1.0	−0.2	0.975559	0.0499368
0.3	0.4	0.959339	−0.0514022	0.7	−1.0	0.415927	0.255948	**1.0**	**0.0**	**1.0**	**0.0**
0.3	0.6	0.910196	−0.0768075	0.7	−0.8	0.577803	0.212813	1.0	0.2	0.975559	−0.0499368
0.3	0.8	0.844452	−0.101833	0.7	−0.6	0.73859	0.163649	1.0	0.4	0.904983	−0.0994785
0.3	1.0	0.764985	−0.126308	0.7	−0.4	0.8755	0.110827	1.0	0.6	0.796175	−0.148144
0.4	−1.0	0.59407	0.20786	0.7	−0.2	0.96755	0.0558974	1.0	0.8	0.661186	−0.195256
0.4	−0.8	0.722508	0.167257	**0.7**	**0.0**	**1.0**	**0.0**	1.0	1.0	0.514615	−0.239762
0.4	−0.6	0.835698	0.125969	0.7	0.2	0.96755	−0.0558974				
0.4	−0.4	0.924252	0.0842184	0.7	0.4	0.8755	−0.110827				

[1] L. Valiant, SIAM J. Comput. **31**, 1229 (2002).

[2] R. Jozsa and A. Miyake, Proc. Royal Soc. A **464**, 3089 (2008).

[3] D. J. Brod and E. F. Galvão, Phys. Rev. A **84**, 022310 (2011).

[4] B. M. Terhal and D. P. DiVincenzo, Phys. Rev. A **65**, 032325 (2002).

[5] D. P. DiVincenzo and B. M. Terhal, Found. Phys. **35**, 1967 (2005).

[6] E. Knill, arXiv:quant-ph/0108033 (2001).

[7] C. W. J. Beenakker, D. P. DiVincenzo, C. Emary, and M. Kindermann, Phys. Rev. Lett. **93**, 020501 (2004).

[8] S. B. Bravyi and A. Y. Kitaev, Ann. Phys. (NY) **298**, 210 (2002).

[9] T. E. O'Brien, P. Rożek, and A. R. Akhmerov, Phys. Rev. Lett. **120**, 220504 (2018).

[10] S. Nadj-Perge, I. K. Drozdov, J. Li, H. Chen, S. Jeon, J. Seo, A. H. MacDonald, B. A. Bernevig, and A. Yazdani, Science **346**, 602 (2014).

[11] V. Mourik, K. Zuo, S. M. Frolov, S. R. Plissard, E. P. A. M. Bakkers, and L. P. Kouwenhoven, Science **336**, 1003 (2012).

[12] S. D. Sarma, M. Freedman, and C. Nayak, npj Quantum Inf. **1**, 15001 (2015).

[13] J. Hubbard and B. H. Flowers, Proc. R. Soc. London Series A: Math. Phys. Sci. **276**, 238 (1963).

[14] A. Georges, G. Kotliar, W. Krauth, and M. J. Rozenberg, Rev. Mod. Phys. **68**, 13 (1996).

[15] P. W. Anderson, Science **235**, 1196 (1987).

[16] D. J. Scalapino, Rev. Mod. Phys. **84**, 1383 (2012).

[17] A. Mazurenko, C. S. Chiu, G. Ji, M. F. Parsons, M. Kanász-Nagy, R. Schmidt, F. Grusdt, E. Demler, D. Greif, and M. Greiner, Nature (London) **545**, 462 (2017).

[18] A. P. Lund, M. J. Bremner, and T. C. Ralph, npj Quantum Inf. **3**, 15 (2017).

[19] I. Bloch, J. Dalibard, and W. Zwerger, Rev. Mod. Phys. **80**, 885 (2008).

[20] A. Görlitz, T. Kinoshita, T. W. Hänsch, and A. Hemmerich, Phys. Rev. A **64**, 011401(R) (2001).

[21] S. Fölling, S. Trotzky, P. Cheinet, M. Feld, R. Saers, A. Widera, T. Müller, and I. Bloch, Nature (London) **448**, 1029 (2007).

[22] M. Köhl, H. Moritz, T. Stöferle, K. Günter, and T. Esslinger, Phys. Rev. Lett. **94**, 080403 (2005).

[23] R. Jördens, N. Strohmaier, K. Günter, H. Moritz, and T. Esslinger, Nature (London) **455**, 204 (2008).

[24] U. Schneider, L. Hackermüller, S. Will, T. Best, I. Bloch, T. A. Costi, R. W. Helmes, D. Rasch, and A. Rosch, Science **322**, 1520 (2008).

[25] H. Moritz, T. Stöferle, K. Günter, M. Köhl, and T. Esslinger, Phys. Rev. Lett. **94**, 210401 (2005).

[26] T. A. Hilker, G. Salomon, F. Grusdt, A. Omran, M. Boll, E. Demler, I. Bloch, and C. Gross, Science **357**, 484 (2017).

[27] B. Song, L. Zhang, C. He, T. F. J. Poon, E. Hajiyev, S. Zhang, X.-J. Liu, and G.-B. Jo, Sci. Adv. **4**, eaao4748 (2018).

[28] M. Boll, T. A. Hilker, G. Salomon, A. Omran, J. Nespolo, L. Pollet, I. Bloch, and C. Gross, Science **353**, 1257 (2016).

[29] L. W. Cheuk, M. A. Nichols, K. R. Lawrence, M. Okan, H. Zhang, and M. W. Zwierlein, Phys. Rev. Lett. **116**, 235301 (2016).

[30] M. F. Parsons, A. Mazurenko, C. S. Chiu, G. Ji, D. Greif, and M. Greiner, Science **353**, 1253 (2016).

[31] L. W. Cheuk, M. A. Nichols, K. R. Lawrence, M. Okan, H. Zhang, E. Khatami, N. Trivedi, T. Paiva, M. Rigol, and M. W. Zwierlein, Science **353**, 1260 (2016).

[32] P. T. Brown, D. Mitra, E. Guardado-Sanchez, P. Schauß, S. S. Kondov, E. Khatami, T. Paiva, N. Trivedi, D. A. Huse, and W. S. Bakr, Science **357**, 1385 (2017).

[33] D. Barredo, S. de Léséleuc, V. Lienhard, T. Lahaye, and A. Browaeys, Science **354**, 1021 (2016).

[34] H. Kim, W. Lee, H.-g. Lee, H. Jo, Y. Song, and J. Ahn, Nat. Commun. **7**, 13317 (2016).

[35] D. Barredo, V. Lienhard, S. de Léséleuc, T. Lahaye, and A. Browaeys, Nature (London) **561**, 79 (2018).

[36] A. Kumar, T.-Y. Wu, F. Giraldo, and D. S. Weiss, Nature (London) **561**, 83 (2018).

[37] D. Ohl de Mello, D. Schäffner, J. Werkmann, T. Preuschoff, L. Kohfahl, M. Schlosser, and G. Birkl, Phys. Rev. Lett. **122**, 203601 (2019).

[38] C. Weitenberg, M. Endres, J. F. Sherson, M. Cheneau, P. Schauß, T. Fukuhara, I. Bloch, and S. Kuhr, Nature (London) **471**, 319 (2011).

[39] E. Haller, J. Hudson, A. Kelly, D. A. Cotta, B. Peaudecerf, G. D. Bruce, and S. Kuhr, Nat. Phys. **11**, 738 (2015).

[40] C. Robens, S. Brakhane, W. Alt, F. Kleißler, D. Meschede, G. Moon, G. Ramola, and A. Alberti, Opt. Lett. **42**, 1043 (2017).

[41] M. McDonald, J. Trisnadi, K.-X. Yao, and C. Chin, Phys. Rev. X **9**, 021001 (2019).

[42] S. Subhankar, Y. Wang, T.-C. Tsui, S. L. Rolston, and J. V. Porto, Phys. Rev. X **9**, 021002 (2019).

[43] G. J. A. Edge, R. Anderson, D. Jervis, D. C. McKay, R. Day, S. Trotzky, and J. H. Thywissen, Phys. Rev. A **92**, 063406 (2015).

[44] M. A. Nichols, L. W. Cheuk, M. Okan, T. R. Hartke, E. Mendez, T. Senthil, E. Khatami, H. Zhang, and M. W. Zwierlein, Science **363**, 383 (2019).

[45] R. A. Hart, P. M. Duarte, T.-L. Yang, X. Liu, T. Paiva, E. Khatami, R. T. Scalettar, N. Trivedi, D. A. Huse, and R. G. Hulet, Nature (London) **519**, 211 (2015).

[46] P. Schauß, J. Zeiher, T. Fukuhara, S. Hild, M. Cheneau, T. Macrì, T. Pohl, I. Bloch, and C. Gross, Science **347**, 1455 (2015).

[47] Y. Y. Jau, A. M. Hankin, T. Keating, I. H. Deutsch, and G. W. Biedermann, Nat. Phys. **12**, 71 (2015).

[48] H. Labuhn, D. Barredo, S. Ravets, S. de Léséleuc, T. Macrì, T. Lahaye, and A. Browaeys, Nature (London) **534**, 667 (2016).

[49] J. Zeiher, R. van Bijnen, P. Schauß, S. Hild, J.-y. Choi, T. Pohl, I. Bloch, and C. Gross, Nat. Phys. **12**, 1095 (2016).

[50] S. Giovanazzi, D. O'Dell, and G. Kurizki, J. Phys. B: At. Mol. Opt. Phys. **34**, 4757 (2001).

[51] S. D. Graham and J. M. McGuirk, Phys. Rev. A **95**, 023602 (2017).

[52] P. Soltan-Panahi, J. Struck, P. Hauke, A. Bick, W. Plenkers, G. Meineke, C. Becker, P. Windpassinger, M. Lewenstein, and K. Sengstock, Nat. Phys. **7**, 434 (2011).

[53] T.-Y. Wu, A. Kumar, F. Giraldo, and D. S. Weiss, Nat. Phys. **15**, 538 (2019).